Fluvial sediment source to sink transfer at the Yellow River Delta: quantifications, causes, and environmental impacts

Hongyu Ji [a,b], Shenliang Chen [a*], Shunqi Pan [a,b], Congliang Xu [c],

Yuanyuan Tian [a,d], Peng Li [a], Qinglan Liu [a], Lijin Chen [a]

[a] State Key Laboratory of Estuarine and Coastal Research, East China Normal University, Shanghai 200241, China.

[b] Hydro-environmental Research Centre, School of Engineering, Cardiff University, Cardiff CF24 3AA, UK.

[c] Institute of the Yellow River Estuary and Coast Science, Dongying 257091, Shandong, China.

[d] School of Geographical Science and Urban Planning, Arizona State University, Tempe, AZ 85281, USA

* Corresponding author.

Email Address: slchen@sklec.ecnu.edu.cn

Highlights

- Geomorphic evolution of the deltaic channel and active river mouth is evaluated.
- Morphologic variability of the active delta has a distinct spatial variance.
- Offshore fine sediment dispersal processes are simulated and quantified.
- The new river regime can improve channel stability and intensify deltaic recession.

Abstract

Intensified human interventions in river basins and deltas lead to more complexities of environmental changes during the Anthropocene. Changes in river regime especially a dramatic reduction in sediment delivery increase challenges of the morphological and ecological sustainability of river deltas. In evaluating deltaic risks and sustainable solutions, researches are often limited to single geomorphic units of the deltaic system, and investigations of sediment source to sink transfer at river deltas under recent river regimes are often missing. The Yellow River Delta (YRD) presents as a typical megadelta under stressors induced by changing environments. This study utilizes a period of 20-yr high-resolution topography data of the deltaic channel and its subaqueous delta to investigate sediment transport and source to sink process by integrated methods of field measurements and numerical simulations. The results indicate that the deltaic channel has transitioned from net accretion to erosion after the implementation of the Water-Sediment Regulation Scheme (WSRS) in 2002. The active river mouth experienced a slow accretion phase since the river channel diverted to Qing 8 channel, with a reduced vertical deposition rate of 0.15 m/yr, whilst its adjacent Gudong littoral zone had a -0.11 m/yr erosion rate. Under the new fluvial regime, the river-borne suspended sediment tends to transport southwards to the Laizhou Bay, followed by the river-derived sediment transport eastward and northward to the offshore delta. It is clear that with the continued human activities in the region, the YRD is at the potential state of deltaic transition both in the deltaic channel and its subaqueous delta. This transition is believed to be beneficial to the deltaic channel stability, but it could significantly impact on the geomorphic and ecologic sustainability of the entire deltaic system.

Keywords

Yellow River Delta; New regime of river delivery; Suspended sediment transport; Source to sink transfer

1. Introduction

Sediment source to sink processes involve transport and dispersal systems of terrestrial sediments from river basins to deep seafloors (Crockett, et al., 2005; Allen, 2008), strongly affecting global material and biogeochemical cycles (Walling and Fang, 2003; Bianchi and Allison, 2009). Among this sediment routing system, river-deltas and their estuaries are one of the critical interfaces where terrestrial inputs emptying into marine environments (Dai et al., 2018). River deltas provide human with habitats to survive, as well as environmental functions such as energy resources, storm protection, carbon storage, and pollution removal (Giosan et al., 2014). During the Anthropocene, river deltas are suffering from erosion risks under the human-altered regime of river delivery, which is largely featured by sediment starvation and river discharge regulation (Syvitski and Saito, 2007; Wang et al., 2006; Best and Darby, 2020). With integrated impacts from other environmental forcing changes including accelerated sea-level rise and frequent storm surges, sediment accumulation rates at low-lying coastal regions cannot keep up with the redistribution and erosional processes from the coastal ocean (Woodroffe et al., 2006; Dunn et al., 2019; Chadwick et al., 2020; Edmonds et al., 2020). In recent decades, the morphological evolution of many megadeltas in the world tends to be in transition from net accretion to erosion, which has been witnessed in the Mississippi (Blum and Roberts, 2009), Yangtze (Yang et al., 2011), Nile (Stanley, 1996), Mekong (Anthony et al., 2015), Ganges-Brahmaputra-Meghna (Wilson and Goodbred, 2015) and Indus deltas (Giosan et al., 2006). The geomorphic transition leads to a potential risk to both deltaic environments and ecosystem survival (Ericson et al., 2006), and a loss of coastal resilience to changing environments (Besset et al., 2019). Thus, sediment transfer processes from source to sink and their geomorphic impacts on river-estuary systems are primary concerns when developing integrated maintenance strategies for delta restoration and future development (Welch et al., 2017; Ogston et al., 2017; Kondolf et al., 2018; Guo et al., 2019).

The Yellow River Delta (YRD), a typical highly human-altered river-delta system, has been in geomorphic adaptions to human engineering interventions and river delivery changes over recent decades. After the Xiaolangdi Reservoir fully operated, the delta accretion rate significantly reduced at both the interannual and decadal scales, due to the dam-induced drastic decline of sediment delivery (Zhou et al., 2015; Jiang et al., 2017; Wu et al., 2017; Fu et al., 2021). The deltaic channel also experienced incision and deepening processes under changing water and sediment supply (Zheng et al., 2018; Han et al., 2020). Groundwater extraction and oil exploitation at the YRD accelerated the land subsidence and shoreline retreat (Higgins et al., 2013; Kuenzer et al., 2014). In addition, river artificial levees were implemented along the delta channel, considering land use and safety, to increase resilience to flooding during extreme flood seasons as well as controlled flood peaks (Syvitski and Saito, 2007; Peng et al., 2010). However, the channel engineering practices have interrupted the exchange of water and sediment between the mainstream and the natural wetlands at the delta plain. Consequently, the natural wetlands are gradually in degradation and replaced by agricultural use.

Sediment transport pathways and sediment budget have been intensively monitored and evaluated in the YRD system since the Qingshuigou became the active deltaic channel. Pang and Si (1980) indicated that during 1964-1973, the deposit ratios of sediment flux at the deltaic channel, subaqueous delta, and to the offshore were 24%, 40% and 36%, respectively. Dong (1997) and Wang (2008) found the multi-year fluvial sediment deposit at the deltaic channel, subaqueous delta and lost to the offshore is 20%, 50% and 30%, respectively. Zhou et al. (2020) indicated that over one-fifth of sediment originated from the Yellow River was transported and deposited at the adjacent Bohai Sea and the Yellow Sea. Bi et al. (2021) assessed a new budget of fluvial sediment dispersal to the sea and found the erosion of abandoned delta lobes as an important sediment source. However, little attention has been paid to quantify the redistribution processes of fluvial sediment from active delta lobe to the coastal ocean since the artificial channel diversion to the current Qing 8 mouth channel in 1996. Furthermore, the offshore sediment transport pathways under the new fluvial regime and current geomorphological settings have rarely been reported.

Hence, the primary goal of this study is to investigate and quantify current fluvial sediment transport and deposition processes along the active YRD lobe and its estuary following the artificial diversion to Qing 8 mouth channel. Specifically, we focus on the sediment dynamics and geomorphic impacts of deltaic channel and the active river mouth, as well as the offshore sediment dispersal patterns. The factors that dominate the sediment transfer processes, and their potential environmental impacts and future geomorphic variability of the YRD are also discussed. This research will shed light on the source to sink transfer of fluvial sediment from the deltaic channel to the sea under the new river regime, and help gain insights into better understand sediment transfer processes of highly human-interfered deltaic systems.

2. Study area

The Yellow River is well known for its high sediment load and suspended sediment concentration (SSC) in its history (Milliman and Meade, 1983). With integrated impacts from human activities and climate change in the river basin, the regime of river delivery has greatly changed, especially since the implementation of WSRS. The new discharge regime is characterized by a more harmonic relationship between water and sediment, with low concentrations of suspended sediment delivery (Yu et al., 2013). It was estimated that dam constructions and soil conservation practices upstream led to over 80% sediment retention in the river basin (Peng et al., 2010). After the implementation of WSRS in 2002, the water discharge remained at a relatively stable level, while the sediment delivered to the sea continued to decrease. The sediment load and annual average SSC at Lijin Station, which is the most seaward hydrological station of the Yellow River, have declined to 1.25×10^8 t/yr and 3.75 kg/m^3 during 2002-2016, respectively.

The modern YRD has experienced frequent channel avulsions and bifurcations since it shifted its course to the Bohai Sea in 1855, forming a fan-shaped and stacked lobe deposition system with over 5400 km^2 deltaic land. Currently, the YRD follows a single deltaic lobe–Qingshuigou lobe since its recent major avulsion in 1976, and the mouth channel was artificially diverted to Qing 8 in 1996 (Figure 1). Strong spatial and temporal variations exist at the YRD due to frequent migrations of the deltaic lobes, with net seaward extension at the active deltaic lobe (Fan et al., 2018) and landward degradation at the abandoned delta (Li et al., 2000). Recently, owing to the insufficient sediment supply, the active river mouth and its adjacent coastal areas experienced reduced accretion (Jiang et al., 2017; Wu et al., 2017), and even severe erosion when the incoming water discharge and sediment load was extremely low, e.g. during the year 2016 (Ji et al., 2018).

The YRD is fluvial-dominated, and most coastal regions have micro-tides with average tidal ranges of 0.73–1.77 m (Yang et al., 2011). The tidal limit is within 30 km and the tidal current limit can only propagate into the deltaic channel within 2–3 km during dry seasons and evolves out of the river mouth during flood seasons (Zhang et al., 2019). Tidal currents are generally parallel to the coastline, which flow southward during flood tide and northward during ebb tide with an average speed of 0.5–1.0 m/s (Bi et al., 2010). The YRD is dominated by northerly wind waves with an average wave height of 0.57 m and an average wave period of 4.3 s as observed during 2006-2019.

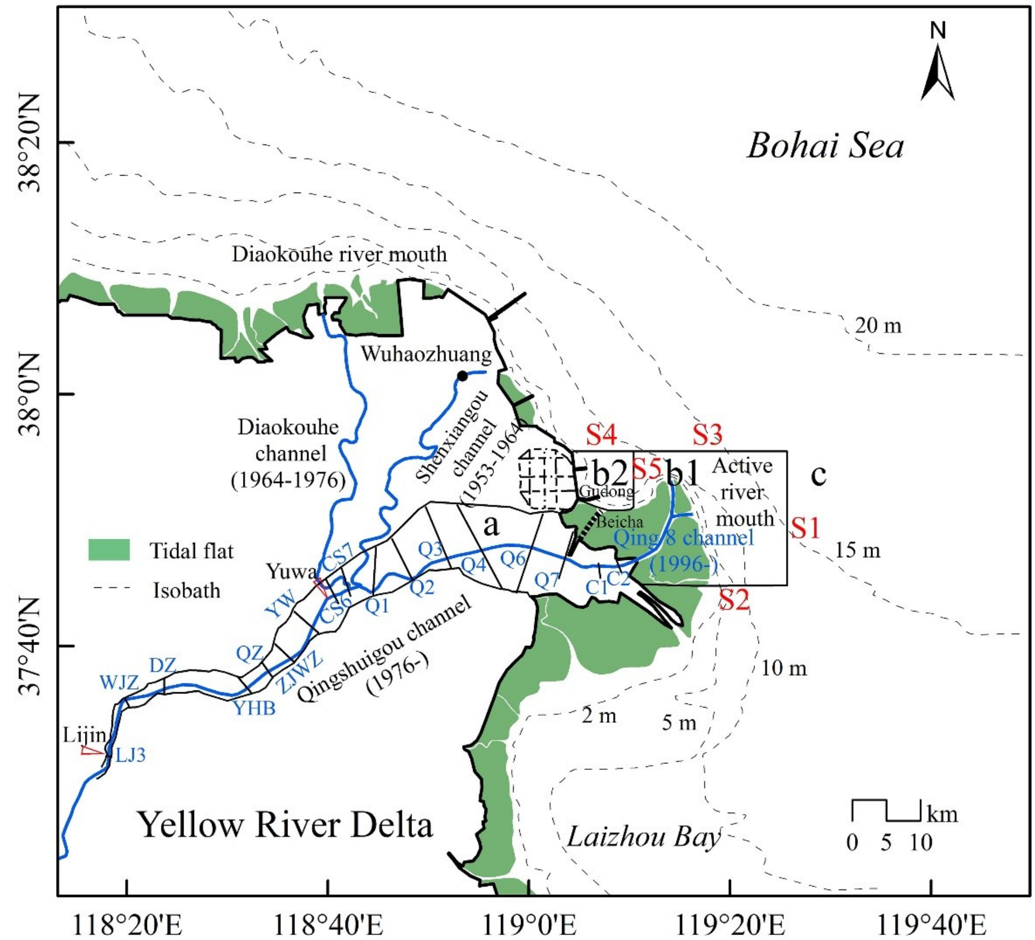

***Figure 1**. Sketch map of the YRD, with study areas in (a) the deltaic channel, (b) the active river mouth and (c) the offshore region. S1-S5 are the representative sections for calculations of net sediment flux.*

The active deltaic lobe and its estuary are highly dynamic geomorphic units, with sensitive response in sediment dynamics under upstream boundary condition changes. Compared with the previous work (Ji et al., 2018), this study expands the study area to the Qingshuigou channel (a), and the active lobe delta, where the active river mouth (b1) and the Gudong littoral zone (b2) are separately discussed based on the field observations of the erosion-accretion patterns (Figure 1). Our primary focus is on the source to sink sediment processes under the control of a single deltaic lobe, and the sediment transport pathways to the offshore delta (c) are elucidated by a full-scale numerical model (Ji et al., 2020). Representative transects S1-S5 are set up to estimate sediment transport pathways and flux (Figure 1).

3. Data and methods

3.1 Data collection

A detailed high-resolution subaqueous topography covering the Yellow River estuary was measured in 1996, 2002, 2007, 2015, and 2018. Different-period topography measurements shared the same range and were precisely measured by SDH-13D digital echo sounder. Accordingly, the remote sensing images in the corresponding years were acquired from the United States Geological Survey Center for Earth Resources Observation and Science (USGS/EROS) to extract waterlines of the delta (Supplementary file Table S1).

The elevation data of 17 cross-sections of the Qingshuigou channel were measured in October in 1996, 2002 and 2016, referring to the Dagu Datum, which is higher than the Yellow Sea Datum of 1.163 m. The cross-sections covered the entire deltaic channel and were spaced from 3 to 8 km (Figure 1; Supplementary file Table S2).

3.2 Method

3.2.1 Erosion-accretion calculation of the deltaic channel and river mouth

Substantial researches have been conducted on the channel geomorphic changes at the YRD (Wang et al, 2006; Zheng et al., 2018; Han et al., 2020; Li et al., 2021). In view of this, this study focuses more on the quantification of sediment dynamics and flux at the deltaic channel since 1996. The volume changes of the deltaic channel can be estimated by the following formula:

$$V_c = \sum_{i=1}^{N-1} \left(\frac{S_i + S_{i+1}}{2}\right) \Delta L_{i,i+1} \tag{1}$$

where, V_c is the total sediment erosion or deposition volume, N is the number of cross-sections, S_i and S_{i+1} are the area changes of the main channel; $\Delta L_{i,i+1}$ is the length of the channel between the i_{th} and $i+1_{\text{th}}$ sections.

To examine the erosion-accretion patterns at certain cross-sections of the deltaic channel, the bankfull area and averaged bed elevation are calculated. The stage of bankfull (Z_{bf}) is often accordant with the discharge that fills a channel to the lips of the active floodplain or farm dikes (Xia et al., 2010). The bankfull area (A_{bf}) is calculated with the horizontal distance of the main channel (W_{bf}) enveloped with the channel geometry (Figure 2). The mean bed elevation (Z_{be}) is calculated as (Han et al., 2020):

$$Z_{be} = Z_{bf} - \frac{A_{bf}}{W_{bf}} \tag{2}$$

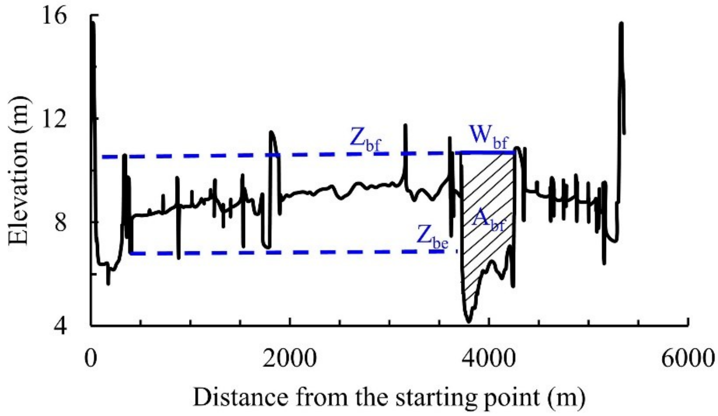

Figure 2. *Schematic diagram for main-channel width W_{bf}, cross-section area A_{bf}, bank elevation Z_{bf} and mean bed elevation Z_{be} at the YW transect shown in Figure 1.*

Fluvial sediment is the main sources to the aggradation of the channel bed and floodplain, as well as the construction of deltaic lobe and the shape of subaqueous delta. The total sediment participating in delta-front building can be considered as the sum of sediment accumulated at the subaerial delta and subaqueous delta. After the artificial diversion at the Qing 8 section in 1996, the active river mouth generally prograded seaward. When comparing topographic changes of the YRD in adjacent years, the shoreline of the previous year was used as the benchmark. Each set of measured bathymetry and shoreline position were interpolated with the Kriging Interpolation technique in 30×30 m resolution (Supplementary file Figure S1). The change of the delta's erosion and deposition volume in the following year relative to the previous year can represent the sum of the erosion and deposition volume of both the subaerial and subaqueous deltas. To estimate the sediment deposition proportions at the subaerial and subaqueous deltas respectively, the shoreline dynamics in the responding years were compared to identify the new-built land, whose elevation was regarded as 0-m (Figure 3).

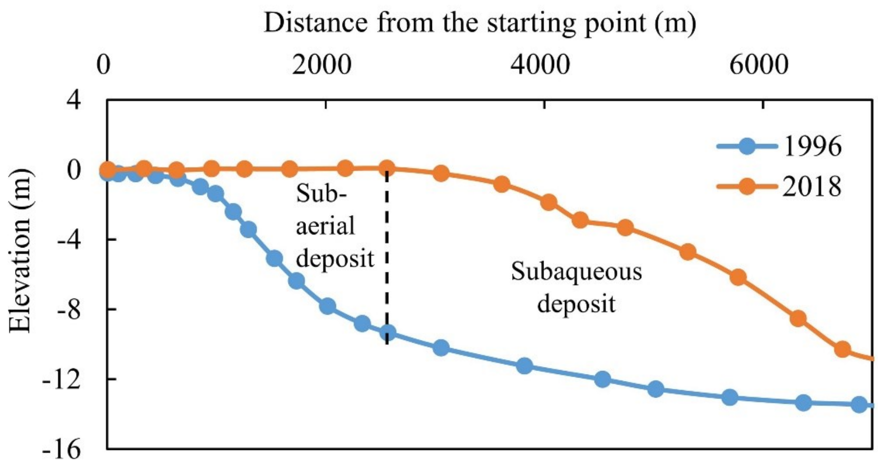

Figure 3. *Sketch map of a topography profile showing land accretion and subaqueous delta deposition process in comparative years, to estimate the sediment deposit proportions in the delta-building.*

3.2.2 Numerical model set-up and validation

A coupled hydrodynamic and sediment transport model of the YRD has been set up for a previous study based on the open-source TELEMAC suite (Ji et al., 2020). Here an introduction of the model set-up and the specific modified parts in the model are given. The hydrodynamic module TELEMAC2D solves the depth-averaged Saint-Venant equations, and the sediment transport module SISYPHE is coupled with TELEMAC2D to compute fine sediment transport at the YRD. It solves the two-dimensional advection-diffusion equation of the suspended sediment concentration (SSC) as:

$$\frac{\partial hC}{\partial t}+\frac{\partial huC}{\partial x}+\frac{\partial hvC}{\partial y}=\frac{\partial}{\partial x}\left(h\varepsilon_s\frac{\partial C}{\partial x}\right)+\frac{\partial}{\partial y}\left(h\varepsilon_s\frac{\partial C}{\partial y}\right)+E-D \qquad (3)$$

where u and v are velocities in x and y direction respectively, C is the depth-averaged SSC, h is the water depth. ε_s is the turbulent diffusivity of the sediment. E and D is the sediment erosion deposition rates respectively, which can be expressed as:

$$D = \alpha\omega C_{Z_{ref}} \quad (4)$$

$$E = \alpha\omega C_{eq} \quad (5)$$

where, $C_{Z_{ref}}$ is the near-bed sediment concentration, C_{eq} is the near-bed equilibrium concentration. ω is the settling velocity, which can be calculated with the following expression for the median sediment grain diameter d_{50} less than 100 μm:

$$\omega = \frac{(s-1)gd_{50}^2}{18} \quad (6)$$

where, s is the relative density of sediment to water. Given the particular characteristics of the fine sediment transported at the YRD, it is necessary to implement a user-defined function in the model to calculate the sediment transport capacity (equal to the near-bed equilibrium concentrations) with the formula proposed by Dou et al. (1995):

$$C_{eq} = \alpha_0 \frac{1}{\omega(s-1)}\left(\frac{r^3 n^2}{h^{\frac{4}{3}}} + \beta_0 \frac{H^2}{hT}\right) \quad (7)$$

where, r is the resultant velocity of u and v, n is Manning's coefficient for bed roughness, s is the specific density of sediment to water. α_0 and β_0 are constants. By considering the complex pattern of sediment size in the study area, a median grain size of 16 μm is chosen to represent the influx of sediment at the upstream boundary.

The computed and observed water levels along the coast of the Bohai Sea and flow velocities and directions near the YRD are compared and validated (Ji et al., 2019; Ji et al., 2020). Here the computed SSC is validated with the in-situ observed SSC in the year 2018 (a1, a2, b1, b2, e1, e2) and 2009 (c1, c2, d1, d2) along the coast of YRD (Figure 4). The observation stations covers the coastal regions from the active river mouth to the northern abandoned YRD.

Figure 5 shows the comparisons of observed SSC and the computed results. It can be seen that the computed SSC generally agrees well with the observations. The high turbidity zone is located at the Qingshuigou river mouth, which can reach over 8 kg/m^3 in flood seasons. The northern YRD is also turbid with about 0.4 kg/m^3 and is largely associated with the weather condition, and the sediment resuspension process can be largely strengthened by wind waves (Fan et al., 2020). It can be also seen that the coastal waters near the Gudong and the Wuhaozhuang are quite clear with low SSC (Figure 5 b1, b2 and c1, c2), because the tidal dynamics and wave actions are relatively weak.

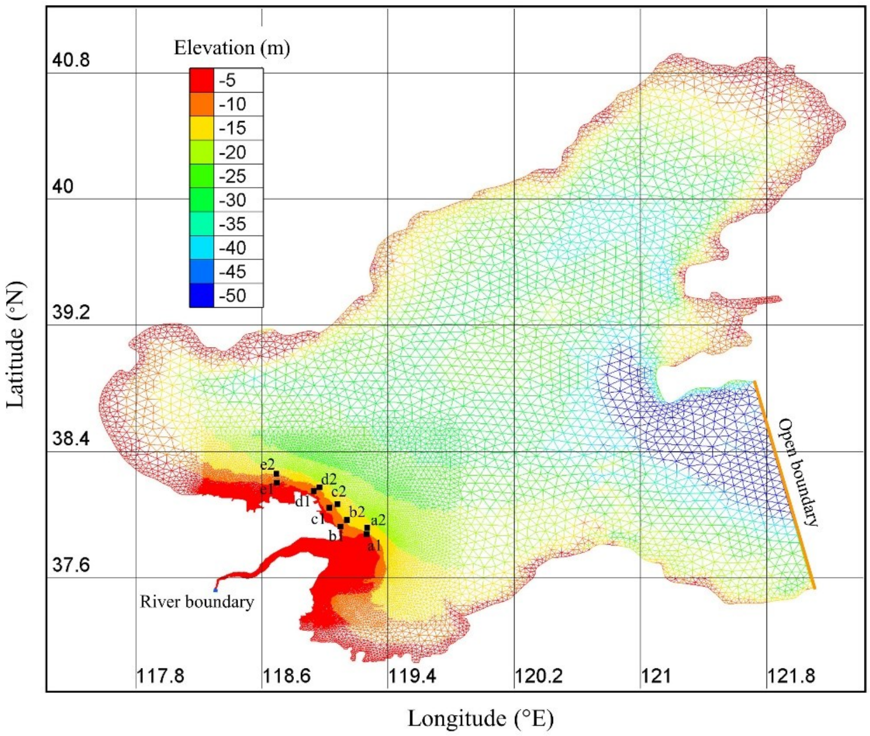

Figure 4. *Computational domain, mesh and locations of field observations near the YRD.*

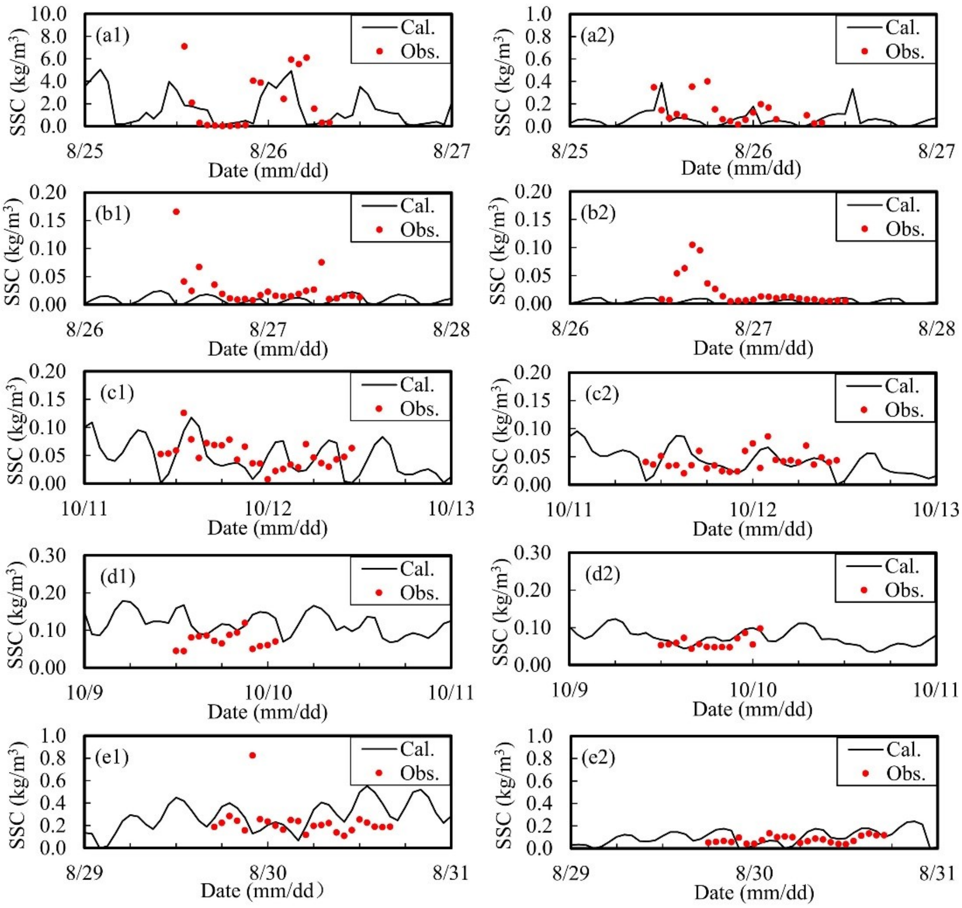

__Figure 5__. Comparisons of the computed and observed SSC.

4. Results

4.1 Sediment budget at the deltaic channel

Since the YRD is fluvial–dominated, the geomorphic evolution of the deltaic channel is closely related to the amount of upstream water and sediment delivery and their relationships (Han et al., 2020). In addition, the sediment dynamics behaviour is active at the main channel rather than over the floodplain even during hyperconcentrated floods, because of the restriction of farm dikes and artificial levees. Under both controlled flood peaks and low flow discharge, the sediment-laden river is rarely overspilled to the floodplain where is now widely covered with paddy fields and marshes (Li et al., 2020; Figure 6).

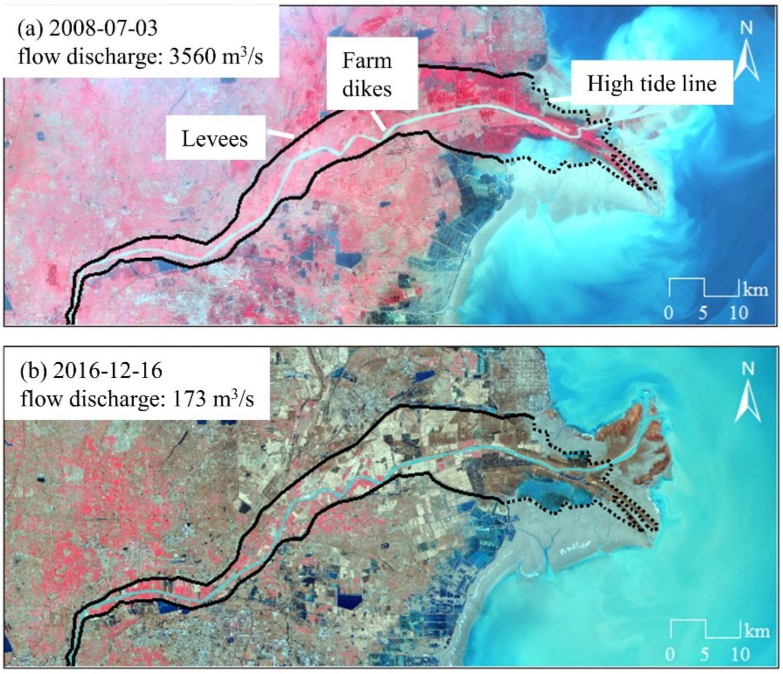

Figure 6. *Satellite images showing the routings of river delivery under different fluvial discharges: (a) high-flow discharge (Landsat-5 band 4/3/2); (b) low-flow discharge (Landsat-8 band 5/4/3).*

Figure 7 shows the topographic changes of 3 selected cross-sections from the upstream towards the mouth of the estuary since 1996. The results indicate a net deposition trend at the deltaic channel before the implementation of WSRS in 2002 and a net erosion trend after. Before 2002, the relationship of water and sediment was imbalanced with a huge amount of sediment delivery and low water discharge input, triggering a rather low sediment transport capacity (Hu, 2005). The upstream incoming sediment tended to deposit at the deltaic channel (Figure 7). After the implementation of WSRS, the relationship between water and sediment became more harmonious with a more drastic decline of sediment load than water discharge. The delivery with low SSC in the river efficiently resulted in scouring the channel bed during 2002-2016, especially during the controlled flood period during the WSRS. It is estimated that the main channel at LJ3 had a net erosion of over 3 m after the implementation of WSRS, whilst the scoured cross-section area reached over 287 m^2. Similarly, the scoured cross-section areas at YW and Q6 amounted 1057 m^2 and 570 m^2 respectively during 2002-2016 (Figure 7).

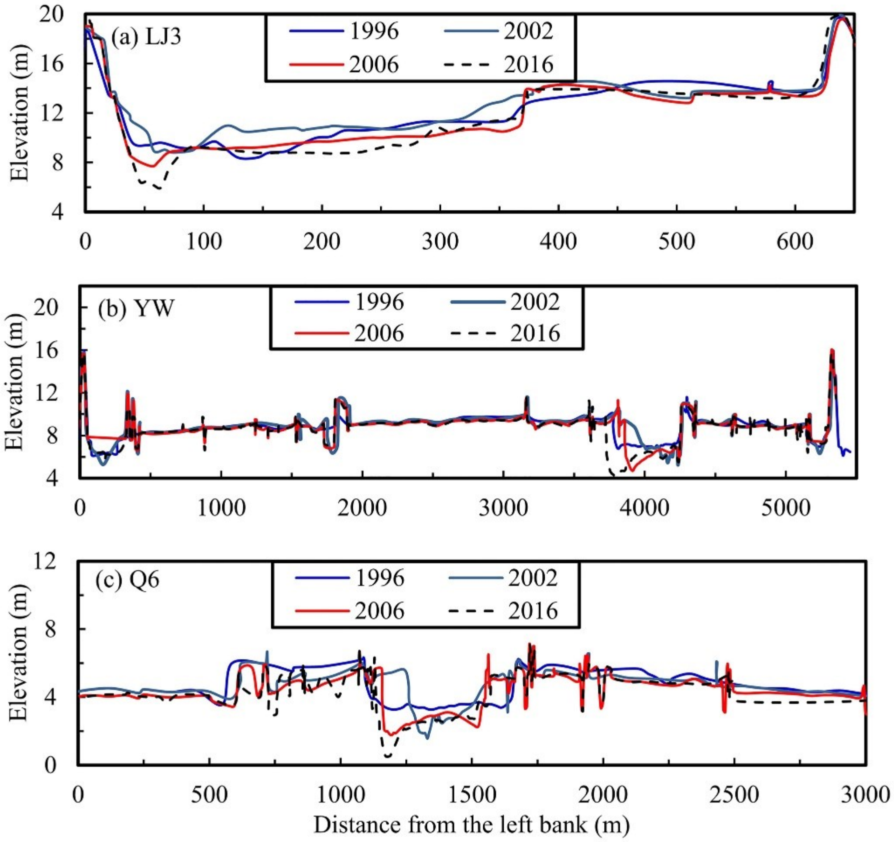

Figure 7. *Morphologic adjustment of the deltaic channel at (a) LJ3, (b) YW and (c) Q6 during 1996-2016.*

An averaged riverbed elevation model of the main deltaic channel was established to investigate the along-channel topographic variations (Supplementary file Table S2). The model results indicated that at the inter-annual scale, the bankfull area of the deltaic channel varied significantly before and after the WSRS operations. From 1996 to 2002, the channel bankfull area generally decreased with a net deposition trend of upstream sediment at the deltaic channel (Figure 8a). Since 2002, the representative cross-sections showed a significant increase of the bankfull area and incision of the main channel, indicating an increased water transport flux and capacity (Figure 8a and b), and an erosion trend at the deltaic channel. By utilizing the channel elevation changes of the 17 cross-sections, the erosion and deposition volume of the riverbed after 1996 was calculated using Eq. 1. The result reveals that the channel bed experienced slight aggradation during 1996-2002 with an deposition volume of 0.14×10^8 m^3. Since 2002, the deltaic channel experienced a rapid erosion with erosion volumes of 0.73×10^8 m^3 during 2002-2006 and 0.37×10^8 m^3 during 2006-2016 (Figure 8c). In total, 1.1×10^8 m^3 of riverbed erosion has occurred since the implementation of the WSRS, accounting for 8.6% of sediment discharge at Lijin Station, which becomes an essential sediment source for the deltaic lobe building, and poses a geomorphic transition from accretion to erosion of the deltaic channel.

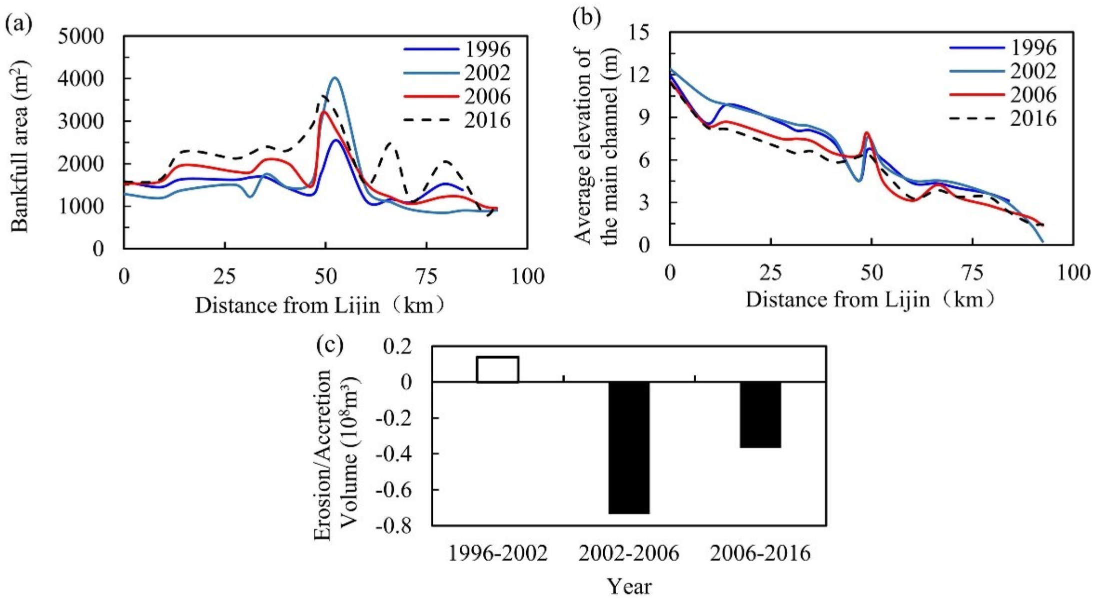

Figure 8. *Erosion-accretion patterns along the Yellow River deltaic channel during 1996-2016: (a) Bankfull area variations; (b) Changes in average elevation of the cross-sections; (c) Erosion and accretion volume of the deltaic channel.*

4.2 Morphologic variability of the active YRD

The Qing 8 channel became the active deltaic channel since the artificial diversion in 1996 and the active river mouth began to rapidly build its land afterward. To depict the erosion-accretion trends of the active delta, we compared the bathymetric changes in 1996, 2002, 2007, 2015 and 2018 over a coastal region of approximately 485 km^2, where most of the upstream sediment was delivered (Wang et al., 2017). The bulk density of sediment used in this study is 1,533 kg/m^3, as suggested by He et al. (2017).

Figure 9 shows the accretion and erosion rates of the active river mouth from 1996 to 2018 in 4 stages. Between 1996 and 2002, the active river mouth experienced net accretion, with a deposition rate of 0.615×10^8 m^3/yr at the active river mouth (Figure 9a). During this period, only 0.032×10^8 m^3/yr of sediment delivery participating in the building process of the subaerial delta. Because the accommodation space for upstream sediment was relatively wide at the initial stage of the new deltaic lobe building, triggering more sediment deposit at the subaqueous portion. At the initial stage of WSRS between 2002 and 2007, the deposition rate reached 0.828×10^8 m^3/yr at the active river mouth, of which only 0.008×10^8 m^3/yr of upstream sediment built the subaerial land (Figure 9b). During 2007-2015, the mouth channel migrated from the eastward to the northward, which triggered the migrations of the depo-center and the erosion-center at the active river mouth (Figure 9c). The depo-center and erosion-center were located within the 10-m depth contour at the active river mouth and the abandoned river mouth, respectively. During 2015-2018, with the decrease of sediment delivery, the deposition rate drastically declined to 0.308×10^8 m^3/yr (Figure 9d; Figure 10). Especially during 2016-2017, the WSRS was interrupted because of the extremely low water and sediment discharge (Ji et al., 2018). Since the artificial diversion of the Qing 8 since 1996, approximately 70.1% of the sediment delivery at Lijin Station was involved in the building of the YRD, and only 23.4% of these sediments participated in the building of the subaerial delta (Supplementary file Table S3).

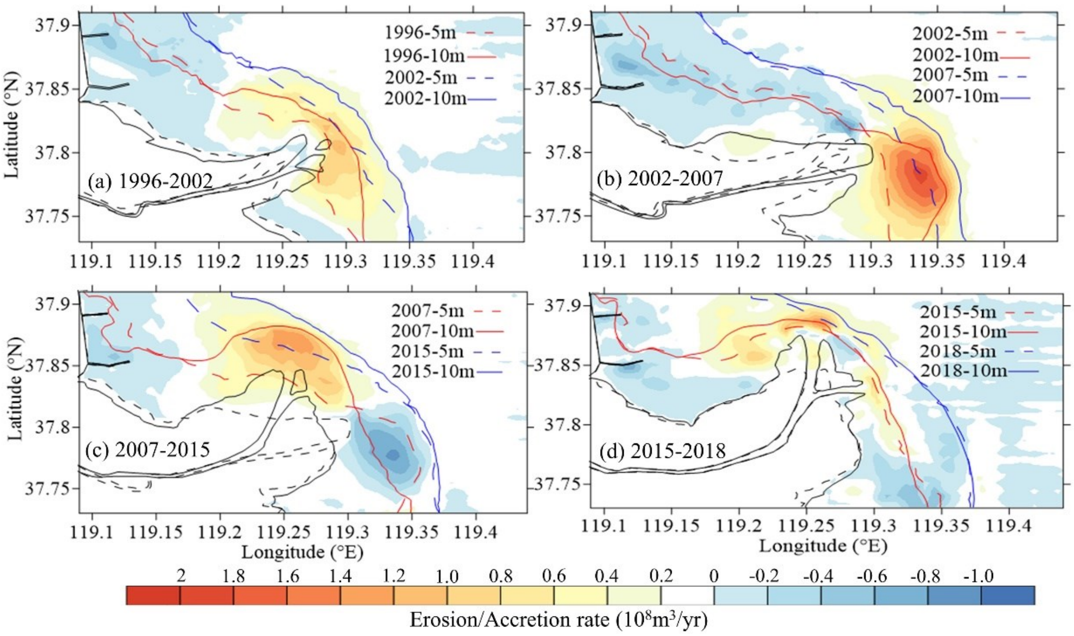

Figure 9. *Accretion and erosion rates of the active river mouth during: (a) 1996-2002, (b) 2002-2007, (c) 2007-2015 and (d) 2015-2018.*

In comparison with both subaerial and subaqueous areas (shown as b1 in Figure 1), the nearshore area in adjacent Gudong littoral zone (shown as b2 in Figure 1) experienced erosion over the entire period between 1996 and 2018 as shown in Figure 10, with severe vertical erosion of -0.11 m/yr. However, in recent years, the erosion rate has decreased due to the migration of the mouth channel from eastward to northward in 2007 (Figure 9c).

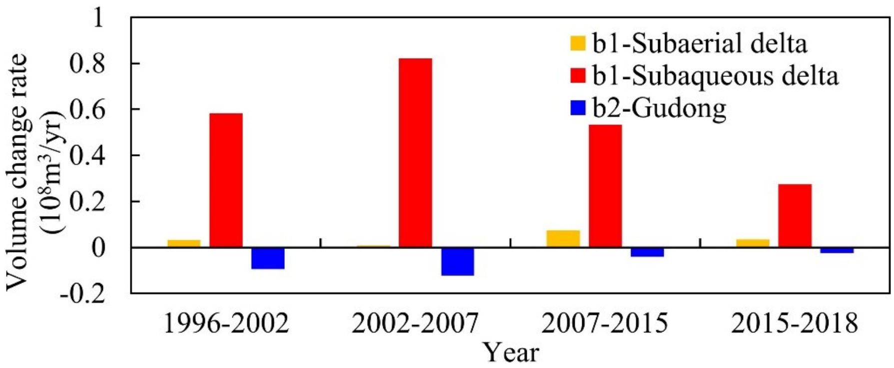

Figure 10. *Erosion and accretion volumes of the areas b1 and b2 at the YRD during 1996-2018. Detailed erosion-accretion patterns can be found in supplementary file Table S3.*

4.3 Sediment transport pathways and flux towards the offshore

Since the implementation of WSRS in 2002, approximately 60.8% of the sediment discharge at Lijin Station participated in the building of the active river mouth. Considering the sediment scoured from the deltaic channel (-8.6%), approximately 47.8 % of upstream sediment tended to transport to the offshore delta (Figure 11). A quantitative analysis of sediment transport pathways and flux were computed from the model results. The net sediment transport flux (*NSTF*) through a transect and the net sediment transport trends (*NSTT*) are calculated by:

$$NSTF = \int_0^T \int_0^L \int_{-H}^{\eta} V(x,y,t)C(x,y,t)dldzdt \quad (8)$$

$$NSTT = \frac{1}{T}\int_0^T \int_{-H}^{\eta} V(x,y,t)C(x,y,t)dzdt \quad (9)$$

where, L is the length of the selected transect, η is the water level, H is the water depth, C is the depth-averaged sediment concentrations, V is the depth-averaged velocities perpendicular to the selected transects, T is the time period considered. Both *NSTF* and *NSTT* were applied to the transects of the subaqueous delta, as well as those outlining the geomorphic feature of the Gudong littoral zone and the active river mouth as shown in Figure 1.

A number of scenarios of the river flow conditions to represent the dynamic forcings were proposed in the investigation. In Case 1, a river discharge of 500 m^3/s was imposed at the river boundary, which represent the average yearly water discharge under the new discharge regime. In Case 2, the river discharge was set to 2000 m^3/s, which represent the average high water flux in flood seasons. In Case 3, the oceanic dynamics including both waves and tides were put into the model. In addition, waves with an averaged height of 1.0 m and a period of 5.0 s were considered to represent the average offshore wave height conditions in the study area. The model was run for two neap-spring tidal cycles to further evaluate the annual net sediment flux through certain transects by Eq. (8).

The result indicates a maximum sediment flux through Section S2. The sediment flux transport through S2 to the Laizhou Bay reaches 0.17×10^8 t/yr and 0.22×10^8 t/yr, respectively, with the river input of 500 m^3/s and 2000 m^3/s imposed at the river boundary (Table 1). The sediment flux through Section S1 reaches $0.036–0.045\times10^8$ t/yr, about 20% of the total southern-dispersal sediment flux. The sediment flux through S3 is 0.03×10^8 t/yr under 500 m^3/s and 2000 m^3/s, which indicates the sediment flux to the north has less relevance with the river input (Table 1). In addition, the sediment flux through sections S4 and S5 is relatively limited.

Table 1. *Quantifications of net sediment flux (10^8t/yr) through representative transects.*

Cases	Dynamics	Scenarios	S1	S2	S3	S4	S5
Case 1	River, Tides	Q=500 m^3/s	0.036	-0.174	0.032	-4.2×10^{-3}	1.8×10^{-4}
Case 2	River, Tides	Q=2000 m^3/s	0.045	-0.220	0.030	-3.9×10^{-3}	1.8×10^{-4}
Case 3	River, Tides and Waves	Q=500 m^3/s, $\overline{H}$=1 m, T=5s	-0.038	-0.630	0.210	0.041	0.013

Note: For sections S1 and S5, the positive value represents net sediment flux to the east, the negative is to the west. For S2, S3 and S4, the positive represents northern transport and the negative represents the sediment transport to the south.

Our calculation of sediment flux through typical transects is quite reliable. In Case 1, the total sediment flux through section S1-S5 is 0.24×10^8 t/yr, accounting for 43.7% of the sediment discharge at the river boundary, which agrees with the geomorphic analysis' estimate of 47.8 % sediment loss to the sea. On the other hand, in Case 3, the computed sediment resuspension at the Gudong littoral zone and transfer to the offshore (through S4 and S5) is 0.054×10^8 t/yr, which is similar to the erosion rate of 0.071×10^8 m^3/yr from the estimations by field observations (Supplementary file Table S3). In both cases, it was clearly demonstrated the consistency of the computational results.

The quantitative result of sediment transport trend is given under the new discharge regime and current geomorphological settings, as shown in Figure 11. Under the 500 m^3/s of water delivery, considering the sediment scoured from the deltaic channel, about 34.4% of upstream sediment discharges to the south (namely Laizhou Bay), 7.1% of sediment transport to the east and 6.3% to the north. It indicates that under normal conditions, the majority of upstream incoming sediment deposits at the active river mouth, and the rest of sediment tends to dispersal southward to the offshore. Comparatively, the sediment transport offshore to the east and the north is relatively limited.

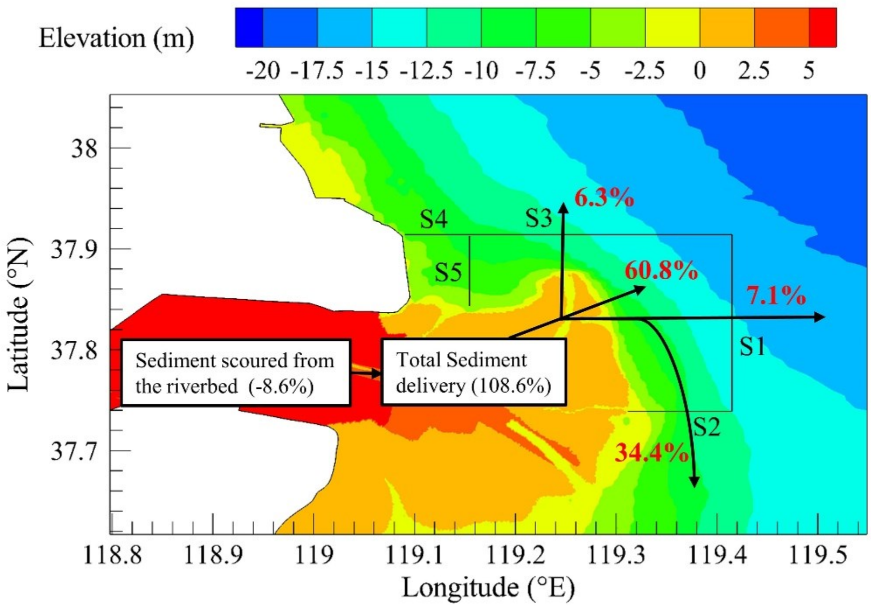

Figure 11. *Quantification of offshore sediment dispersal trends through sections S1-S5 relative to the sediment discharge at Lijin Station.*

5. Discussions

5.1. Spatial-temporal variations of deltaic accretion and erosion

Reduced sediment supply induces transition in geomorphic evolution processes at the active YRD from rapid accretion to reduced accretion state. During 1986-1996, a depo-center with net siltation larger than 6-m was formed at the Qingshuigou river mouth, with an area of 183.06 km^2 (Jiang et al., 2017). It drastically shrank to 54.3 km^2 during 1996-2018, which indicated a significant decrease in deposition flux at the active river mouth (Figure 12). Although the active river mouth and Gudong littoral zone are geographically adjacent, strong spatial heterogeneity in geomorphic evolution is observed. Since the Qing 8 section became the active mouth channel, the active river mouth was at net depositional state with a vertical accretion rate of 0.15 m/yr, whereas the Gudong littoral zone experienced a severe erosion with -0.11 m/yr.

From the perspectives of tide dynamics, the strong shore-parallel tidal currents and the tidal shear front developed at the active river mouth act as a barrier to the sediment dispersal, thus triggering a rapid deposition rate at the active river mouth (Wang et al., 2017; Ji et al., 2020). In addition, the salinity front led by baroclinic transport also restricts the fine sediment transport out of the estuary (Cheng et al., 2021). It induces the active river mouth as a depo-center since the artificial diversion in 1996, and the depo-center tends to be restricted in the shallow waters within the 10-m depth contour (Figure 12).

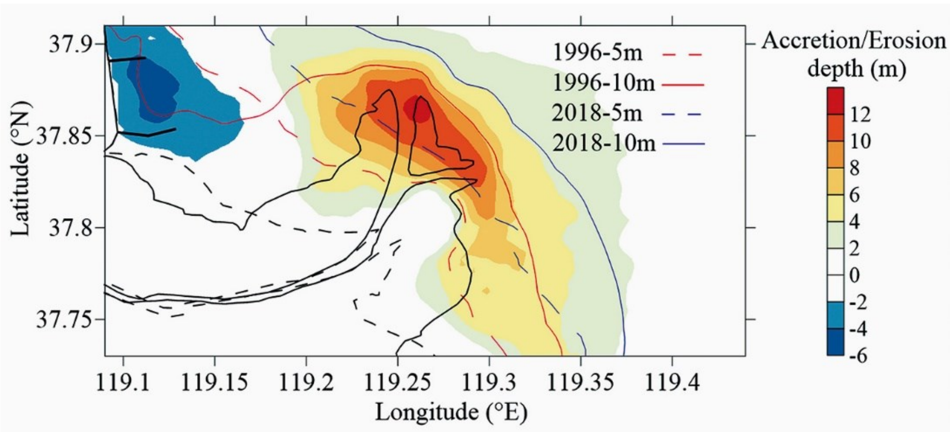

Figure 12. *Erosion-accretion patterns at the active YRD during 1996-2018.*

To better understand the dynamic mechanism of the continuous erosion of the Gudong littoral zone, Figure 13 shows the net sediment flux computed for Case 1 and Case 3 by Eq. (9) When considering the river-tide dynamics in Case 1, the riverine sediment flux tends to transport to the south off the river mouth and the net sediment flux per width could reach 0.2 kg/s near the river mouth (Figure 13a). Compared to the southern transport of the fine sediment, less fluvial sediment transport northerly and can barely transport to the Gudong littoral zone because there is a counterclockwise vortex of net sediment flux around the erosion-accretion transition zone (Figure 13a). Although there is sediment supply originated from the northern Gudong by the integrated impact of the tide-induced and wave-induced sediment resuspension, the amount is comparably quite limited. When considering the combined effects of river, tide and wave actions in Case 3, a similar tendency of sediment transport patterns at the active river mouth can be seen in Figure 13b. Furthermore, the sediment has both northernly and easternly transport trends near the Gudong littoral zone, which matches well the field observations.

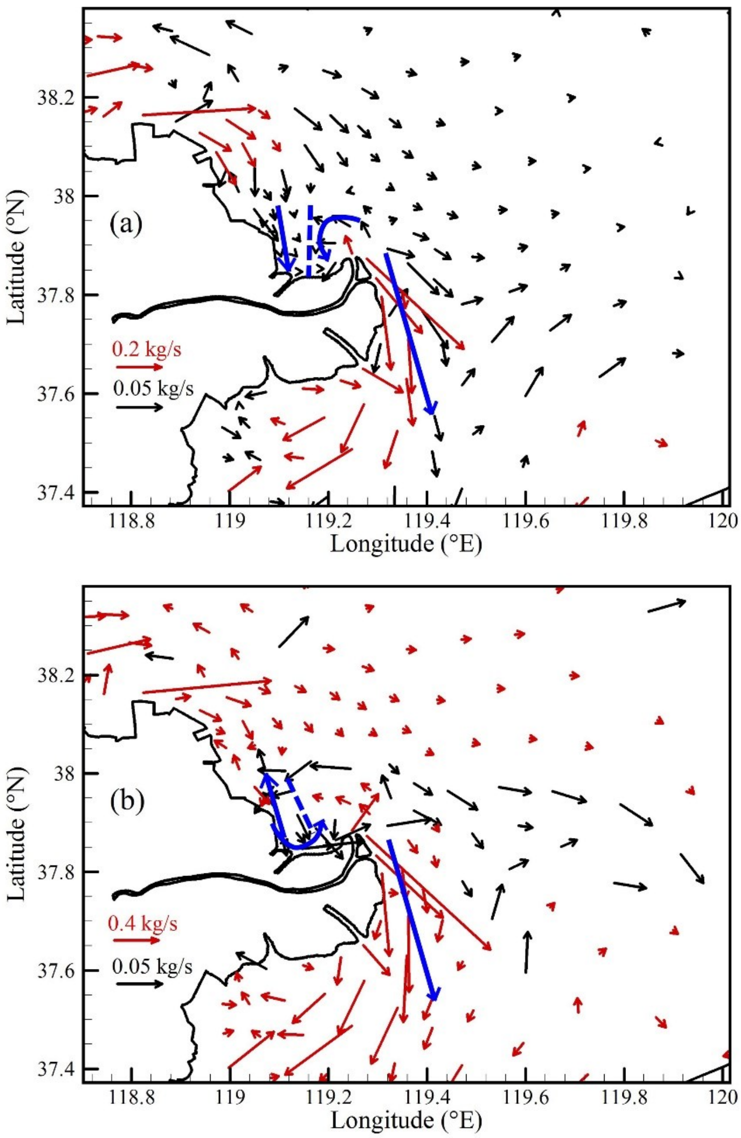

Figure 13. *Net sediment flux under the combined influence of (a) river-tide dynamics, and (b) river-tide-wave dynamics at the YRD. The blue arrows indicate the directions of sediment transport trend and the blue dash line is the transition zone of erosion and accretion between the active river mouth and the Gudong littoral zone.*

5.2. Causes for geomorphic transition of the YRD and its environmental impacts

Sediment transport pathways and flux at river deltas strongly depend on the shifts of the active delta lobe, coastal ocean dynamics, and incoming water and sediment regimes such as sediment grain size and river discharge (Fagherazzi et al., 2015; Bi et al., 2021). The sediment dynamics along the delta plain and the river mouth have received significant attention, particularly before the artificial diversion at Qing 8 Section. Between 1958-1979, the proportions of upstream sediment deposition at the deltaic channel, the active river mouth and towards offshore was estimated to be 20%, 50% and 30%, respectively relative to the sediment discharge measured at Lijin Station (Pang and Si, 1980; Dong, 1997) as listed in Table 2. Following the mouth channel migration and basin-scale water regulation, the delta-building processes of the active river mouth began and the sediment source to sink processes of the YRD shifted thereafter. The deltaic channel experienced a slight deposition state, between 1996 and 2002, with 0.22×10^{8} t of sediment deposition. Near the active river mouth, there was a huge accommodation space with very efficient sediment trapping capability. The deposition ratio, sediment entrapment out of the total incoming sediment from the upstream, reached 73.5%. The geomorphic transition in the deltaic channel is detected since the implementation of the WSRS. Under the new discharge regime, 8.6% of sediment discharge into the sea was estimated to be eroded from the deltaic channel after the WSRS, 60.8% of sediment discharge at Lijin

Station participated in the direct building of the YRD, and the remaining 47.8% tended to transport offshore (Table 2).

Table 2. *Distribution of sediment deposition at the deltaic channel, subaqueous delta and transport to the offshore, modified from Pang and Si (1980) and Dong (1997).*

Period	Deltaic channel (%)	River mouth (%)	Offshore delta (%)
Shenxiangou channel（1958-1960）	3.6	45.5	50.9
Diaokouhe channel（1964-1973）	24.0	40.0	36.0
Qingshuigou channel（1976-1979）	32.9	44.6	22.5
Qing 8 Channel（1996-2002）	**2.9**	**73.5**	**23.6**
After WSRS（2002-2018）	**-8.6**	**60.8**	**47.8**

The geomorphic transition of the active deltaic channel and river mouth is closely associated with the regime changes in water and sediment delivery (Wang et al., 2017; Han et al., 2020). The basin-scale WSRS has shifted the imbalanced relationship between water and sediment discharge, with coarser sediment delivery and low suspended sediment concentrations delivered to the YRD (Ji et al., 2018). Each year from late-June to mid-July after the WSRS was implemented, the controlled floodwaters have sufficiently scoured the riverbed of the downstream channel (Bi et al., 2019). The delta-building processes are aided by scoured riverbed material delivered to the sea. With the combined impacts from the delivery of coarse sediment scoured from the downstream riverbed, the deposition rate of total sediment delivery at the active river mouth significantly increased compared to that before 1996. However, the insufficient sediment supply, which substantially dropped since 2002, remained the dominant factor in shaping deltaic transition from rapid deposition to reduced accretion. In the non-flood seasons, the deltaic channel experienced net deposition and the active river mouth entered an erosion state (Liu et al., 2021). Thus from both intra-annual to inter-annual scales, the riverine regime changes induced by WSRS shift the sediment source to sink transfer processes of the active YRD system from the deltaic channel to the active river mouth.

The geomorphic transition has crucial environmental impacts on the deltaic system as follows:

(1) With the single active deltaic channel, the coastal areas that upstream riverine flow can benefit from are limited (Wang et al., 2019). The reduced water and sediment supply as well as land reclamation projects reduce water accessibility (Li et al., 2000), especially in the oil field zone and the erosion zone at the northern YRD far from the active lobe (Xie et al., 2020), which may exacerbate coastal wetland loss and ecological degradation.

(2) The sediment-laden river flows through the floodplain and has frequent avulsions and bifurcations when heavy sediment load is delivered at the upstream boundary (Zheng et al., 2018). The Qingshuigou lobe has stabilized its paths since 1976 and alters the upstream inflow condition, which is characterized by reduced sediment delivery and low SSC. This benefits the deepening and maintenance of the deltaic channel because the water regulation was implemented in 2002 and the geomorphic transition of the deltaic channel.

(3) Under the new discharge regime, the geomorphic evolution of the YRD has a distinct spatial variance, which is dominated by reduced accretion at the active lobe river mouth and continuous erosion at the abandoned delta lobe. Even in extremely dry years, the active delta also experienced severe erosion (Ji et al., 2018). Coastal erosion of the deltaic system would inevitably increase coastal vulnerability and dike breach risk in the engineering protection zone. It was reported that the two typhoon events in 1992 and 1997 directly caused about 970 million CNY loss to the local oilfield (Chen et al., 2006).

5.3. Potential geomorphic evolution of the future Yellow River deltaic system

The YRD presents as a typical mega-river deltaic system under intensive human activities and sediment starvation. Under the new regime of river delivery since 2002, we analyzed the source to sink transfer of terrestrial sediment at the YRD and potential transport pathways at adjacent coastal waters. It is uncovered that the deltaic channel has transitioned from the accretion to the erosion state, and the active river mouth has experienced rapid deposition to reduced accretion since the WSRS came into operation.

Human interference at river basin including dam construction, the WSRS as well as high-intensity soil and water conservation practice, is regulating the Yellow River into a highly human-altered mega-river system, and it is to some extent irreversible. From the current stage of geomorphic evolution, if the highly human-altered fluvial regime and the single active lobe sustain, the erosion trend of the deltaic system is expected to continue. Other environmental forcings, including accelerated sea-level rise, land subsidence and frequent storm surges, can inevitably intensify the coastal erosion of the YRD (BCSL, 2010; Higgins et al., 2013; Fan et al., 2020).

Studies have revealed that the basin-scale water regulation is efficient in riverbed scouring of the lower Yellow River, but it needs potential improvement in maintaining the coastal resilience of the YRD due to the insufficient sediment supply (Wu et al., 2021). To cope with the deltaic transition, Yu et al. (2020) revealed the Beicha (see Figure 1) as the alternate flow path by considering the channel stability and the relief of erosion at the Gudong littoral zone. Our study shows the integrated regulation strategies including water regulation and channel migration need to be carefully considered and appropriately formulated, which should prioritize both the geomorphic and environmental implications for the lower reach of the river and future development of the deltaic system.

6. Conclusions

In this study, a quantitative analysis of the sediment source to sink process at the YRD is carried out, by a holistic analysis of channel topography, subaqueous delta bathymetry and numerical simulations. A sediment budget of the deltaic system including the deltaic channel, the active mouth, as well as the sediment dispersal pathways towards the offshore is also quantified. Since the implementation of the basin-scale WSRS, the deltaic channel has transitioned from net accretion to erosion state. Its erosion volume reaches 1.1×10^8 m^3, constituting approximately 8.6% of total sediment amount passing Lijin Station, becoming an essential sediment source for deltaic lobe building. The morphological variability of the active river mouth was closely associated with the regime of river delivery and mouth channel migrations, and generally experienced a reduced accretion trend since the Qing 8 became the active mouth channel. As a result of the starvation of sediment supply and strong wave actions, the Gudong littoral zone has experienced continuous erosion. A preliminary quantitative analysis of sediment transport pathways shows approximately 34.4% of the sediment discharge at Lijin Station delivered to the sea transport to the south, 7.1% of sediment transport to the east and 6.3% to the north, and river-derived sediment hardly reach the adjacent Gudong littoral zone. Under the single active deltaic channel and highly human-altered river regime at the inflow boundary, the future YRD is expected to keep on the reduced accretion of the active river mouth, and maintain erosion state of both the deltaic channel and the Gudong littoral zone. This geomorphic evolution has potential environmental impacts on exacerbating the coastal wetland loss, ecological degradation and coastal vulnerability.

Declaration of Competing Interest

The authors declared that there is no conflict of interest with third parties.

Acknowledgments

This study was partly supported by the National Science Foundation of China (NSFC, No.U1706214), the National Key Research and Development Program of China (No.2017YFC0405503), the Open Research Fund of SKLEC (SKLEC-PGKF201903, SKLEC-KF202001), and the joint Ph.D. program of the China Scholarship Council for Overseas Studies (No. 201806140079). We would also link to acknowledge the Yellow River Conservancy Commission, Ministry of Water Resources of China for providing the hydrographic data, as well as the open-source remote sensing data provided by the USGS. We would also thank editor and reviewers for their insightful and constructive comments.

Appendix A. Supplementary data

Supplementary data consist of Table S1-S3 and Figure S1, including information of bathymetric surveys at the deltaic channel and the subaqueous delta, and a detailed erosion-accretion volume of the active lobe delta vicinity during 1996-2018.

References

Allen, P.A., 2008. From landscapes into geological history. Nature, 451(7176): 274-276.

Anthony, E.J., Brunier, G., Besset, M., Goichot, M., Dussouillez, P., Nguyen, V.L., 2015. Linking rapid erosion of the Mekong River delta to human activities. Scientific Reports, 5: 14745.

Besset, M., Anthony, E.J, Bouchette, F., 2019. Multi-decadal variations in delta shorelines and their relationship to river sediment supply: An assessment and review. Earth-science reviews, 193: 199-219.

Best, J., Darby, S.E., 2020. The pace of human-induced change in large rivers: Stresses, resilience, and vulnerability to extreme events. One Earth, 2(6): 510-514.

Bi, N., Sun, Z., Wang, H., et al., 2019. Response of channel scouring and deposition to the regulation of large reservoirs: A case study of the lower reaches of the Yellow River (Huanghe). Journal of Hydrology, 568: 972-984.

Bi, N., Wang, H., Wu, X., Saito, Y., Xu, C., Yang, Z., 2021. Phase change in evolution of the modern Huanghe (Yellow River) Delta: Process, pattern, and mechanisms. Marine Geology, 437: 106516.

Bianchi, T.S., Allison, M.A., 2009. Large-river delta-front estuaries as natural "recorders" of global environmental change. Proceedings of the National Academy of Sciences of the United States of America, 106(20): 8085-92.

Blum, M.D., Roberts, H.H., 2009. Drowning of the Mississippi Delta due to insufficient sediment supply and global sea-level rise. Nature Geoscience, 2(7): 488-491.

Bulletin of China Sea Level (BCSL), 2010. State Oceanic Administration.

Chadwick, A.J., Lamb, M.P., Ganti, V., 2020. Accelerated river avulsion frequency on lowland deltas due to sea-level rise. Proceedings of the National Academy of Sciences, 117(30): 17584-17590.

Chen, S., Zhang, G., Chen, X., 2006. Coastal erosion feature and mechanism at Feiyantan in the Yellow River Delta. Marine Science Bulletin, 8(1):11-21.

Cheng, X., Zhu, J., Chen, S., 2021. Extensions of the river plume under various Yellow River courses into the Bohai Sea at different times. Estuarine, Coastal and Shelf Science, 249: 107092.

Crockett, J.S., Nittrouer, C.A., Ogston, A.S., Sternberg, R.W., Driscoll, N.W., Babcock, J., Milliman, J.D., Slingerland, R., Naar, D.F., Donahue, B., Walsh, J.P., Dietrich, W., Parker, G., Bera, M., Davies, H., Harris, P., Goni, M., Aller, R., Aller, J., 2005. Where rivers and oceans collide. Eos, Transactions American Geophysical Union, 86(3): 25-32.

Dai, Z., Mei, X., Darby, S.E., Lou, Y., Li, W., 2018. Fluvial sediment transfer in the Changjiang (Yangtze) river-estuary depositional system. Journal of Hydrology, 566: 719-734.

Dong, N., 1997. The deposit and diffuse of the Yellow River sediment into the sea. The Ocean Engineering, 15(2): 59-64. (In Chinese)

Dou, G., Dong, F., Dou, X., Li, T., 1995. Mathematical modeling of sediment transport in estuaries and coastal regions. Science in China (Series A), 38(10), 1251-1260.

Dunn, F.E., Darby, S.E., Nicholls, R.J., Cohen, S., Zarfl, C., Fekete, B.M., 2019. Projections of declining fluvial sediment delivery to major deltas worldwide in response to climate change and anthropogenic stress. Environmental Research Letters, 14(8): 084034.

Edmonds, D.A., Cardwell, R.L., Brondizio, E.S., Siani, S.M.O., 2020. Coastal flooding will disproportionately impact people on river deltas. Nature Communications, 11: 4741.

Ericson, J.P., Vörösmarty, C.J., Dingman, S.L., Ward, L.G., Meybeck, M., 2006. Effective sea-level rise and deltas: Causes of change and human dimension implications. Global and Planetary Change, 50(1-2): 63-82.

Fagherazzi, S., Edmonds, D.A., Nardin, W., Leonardi, N., Canestrelli, A., Falcini, F., Jerolmack, D.L., Mariotti, G., Rowland, J.C., Slingerland, R.L., 2015. Dynamics of river mouth deposits. Reviews of Geophysics, 53(3): 642-672.

Fan, Y., Chen, S., Zhao, B., Pan, S., Jiang, C., Ji, H., 2018. Shoreline dynamics of the active Yellow River delta since the implementation of Water-Sediment Regulation Scheme: A remote-sensing and statistics-based approach. Estuarine, Coastal and Shelf Science, 200: 406-419.

Fan, Y., Chen, S., Pan, S., Dou, S., 2020. Storm-induced hydrodynamic changes and seabed erosion in the littoral area of Yellow River Delta: A model-guided mechanism study. Continental Shelf Research, 205:104171

Fu, Y., Chen, S., Ji, H., Fan, Y., Li, P., 2021. The modern Yellow River Delta in transition: Causes and implications. Marine Geology, 436: 106476.

Giosan, L., Constantinescu, S., Clift, P.D., Tabrez, A.R., Danish, M., Inam, A., 2006. Recent morphodynamics of the Indus delta shore and shelf. Continental Shelf Research, 26(14): 1668-1684.

Giosan, L., Syvitski, J.P.M., Constantinescu, S., Day, J., 2014. Climate change: Protect the world's deltas. Nature, 516: 31-33.

Guo, L., Su, N., Townend, I., Wang, Z., Zhu, C., Wang, X., Zhang, Y., He, Q., 2019. From the headwater to the delta: A synthesis of the basin-scale sediment load regime in the Changjiang River. Earth-Science Reviews, 197: 102900.

Han, S., Rice, S., Tan, G., Wang, K., Zheng, S., 2020. Geomorphic evolution of the Qingshuigou channel of the Yellow River Delta in response to changing water and sediment regimes and human interventions. Earth Surface Processes and Landforms, 45(10): 2350-2364.

He, C., Li, X., Zuo, X., 2017. Analysis and research on sediment bulk density test in coastal area of Yellow River estuary. Water Resources Development and Management (4): 70-72. (In Chinese with English Abstract)

Higgins, S., Overeem, I., Tanaka, A., Syvitski, J.P.M., 2013. Land subsidence at aquaculture facilities in the Yellow River delta, China. Geophysical Research Letters, 40(15): 3898-3902.

Hu, C., 2005. Variation of flow and sediment and complicated response of channels in the Yellow River. Beijing: The publishing company of science.

Kondolf, G.M., Schmitt, R.J.P., Carling, P., Darby, S., Arias, M., Bizzi, S., Castelletti, A., Cochrane, T.A., Gibson, S., Kummu, M., Oeurng, C., Rubin, Z., Wild, T., 2018. Changing sediment budget of the Mekong: Cumulative threats and management strategies for a large river basin. Science of the Total Environment, 625: 114-134.

Kuenzer, C., Ottinger, M., Liu, G., Sun, B., Baumhauer, R., Dech, S., 2014. Earth observation-based coastal zone monitoring of the Yellow River Delta: Dynamics in China's second largest oil producing region over four decades. Applied Geography, 55: 92-107.

Ji, H., Chen, S., Pan, S., Xu, C., Jiang, C., Fan, Y., 2018. Morphological variability of the active Yellow River mouth under the new regime of riverine delivery. Journal of Hydrology, 564: 329-341.

Ji, H.., Pan, S., Chen, S., Jiang, C., 2019. Impact of riverine delivery on tidal dynamics of Yellow River Delta. E-proceedings of the 38th IAHR World Congress, September 1-6, 2019, Panama City, Panama. 3032-3041.

Ji, H., Pan. S., Chen, S., 2020. Impact of river discharge on hydrodynamics and sedimentary processes at Yellow River Delta. Marine Geology, 425: 106210.

Jiang, C., Pan, S., Chen, S., 2017. Recent morphological changes of the Yellow River (Huanghe) submerged delta: Causes and environmental implications. Geomorphology, 293: 93-107.

Li, G., Zhuang, K., Wei, H., 2000. Sedimentation in the Yellow River delta. Part III. Seabed erosion and diapirism in the abandoned subaqueous delta lobe. Marine Geology, 168(1): 129-144.

Li, H., Fan, Y., Gong, Z., Zhou, D., 2020. Water accessibility assessment of freshwater wetlands in the Yellow River Delta National Nature Reserve, China. Ecohydrology & Hydrobiology, 20(1): 21-30.

Li, J., Xia, J., Ji, Q., 2021. Rapid and long-distance channel incision in the Lower Yellow River owing to upstream damming. Catena, 196:104943.

Liu, Q., Chen, J., Chen, S., 2021. Spatiotemporal evolution of Yellow River estuarine channel and its influencing factors since the water-sediment regulation scheme. Acta Geographica Sinica, 76(1): 1-14.

Milliman, J.D., Meade, R.H., 1983. World-wide delivery of river sediment to the oceans. The Journal of Geology, 91(1): 1-21.

Ogston, A.S., Allison, M.A., McLachlan, R.L., Nowacki, D.J., Stephens, J.D., 2017. How tidal processes impact the transfer of sediment from source to sink: Mekong River collaborative studies. Oceanography, 30(3): 22-33.

Pang, J., Si, S., 1980. Fluvial process of the Huanghe River Estuary: Ⅱ Hydrographical character and the region of sediment silting. Oceanologia Et Limnologia Sinica, 11(4):

295-305. (In Chinese)

Peng, J., Chen, S., Dong, P., 2010. Temporal variation of sediment load in the Yellow River basin, China, and its impacts on the lower reaches and the river delta. Catena, 83(2-3): 135-147.

Stanley, D.J., 1996. Nile delta: extreme case of sediment entrapment on a delta plain and consequent coastal land loss. Marine Geology, 129(3): 189-195.

Syvitski, J.P.M., Saito, Y., 2007. Morphodynamics of deltas under the influence of humans. Global and Planetary Change, 57(3-4): 261-282.

Walling, D.E., Fang, D., 2003. Recent trends in the suspended sediment loads of the world's rivers. Global and Planetary Change, 39: 111-126.

Wang, C., Cao, W., Zhang, S., 2008. Tidal current and sediment transport capacity in Yellow River estuary. Journal of Hydraulic Engineering, 39(10): 1256-1263. (In Chinese)

Wang, H., Yang, Z., Saito, Y., Liu, J.P., Sun, X., 2006. Interannual and seasonal variation of the Huanghe (Yellow River) water discharge over the past 50 years: Connections to impacts from ENSO events and dams. Global and Planetary Change, 50: 212-225.

Wang, H., Wu, X., Bi, N., Li, S., Yuan, P., Wang, A., Syvitski, J.P.M., Saito, Y., Yang, Z., Liu, S., Nittrouer, J., 2017. Impacts of the dam-orientated water-sediment regulation scheme on the lower reaches and delta of the Yellow River (Huanghe): A review. Global and Planetary Change, 157: 93-113.

Wang, J., Hu, P., Gong, J., 2019. Taking the great protection of the Yellow River Estuary as the grasp to promote the construction of ecological civilization of in the Yellow River basin. Yellow River, 41(10): 7-10. (in Chinese)

Wang, N., Li, G., Qiao, L., Shi, J., Dong, P., Xu, J., Ma, Y., 2017. Long-term evolution in the location, propagation, and magnitude of the tidal shear front off the Yellow River Mouth. Continental Shelf Research, 137: 1-12.

Wang, S., Hassan, M.A., Xie, X., 2006. Relationship between suspended sediment load, channel geometry and land area increment in the Yellow River Delta. Catena, 65(3): 302-314.

Welch, A.C, Nicholls, R.J., Lázár, A.N., 2017. Evolving deltas: Coevolution with engineered interventions. Elementa: Science of the Anthropocene, 5: 49.

Wilson, C.A., Goodbred, S.L., Jr., 2015. Construction and maintenance of the Ganges-Brahmaputra-Meghna delta: linking process, morphology, and stratigraphy. Annual Review of Marine Science, 7: 67-88.

Woodroffe, C.D., Nicholls, R.J., Saito, Y., Chen, Z.Y., Goodbred, S.L., 2006. Landscape Variability and the Response of Asian Megadeltas to Environmental Change. Coastal Systems and Continental Margins, 10: 277-314.

Wu, X., Bi, N., Xu, J., Nittrouer, J.A., Yang, Z., Saito, Y., Wang, H., 2017. Stepwise morphological evolution of the active Yellow River (Huanghe) delta lobe (1976–2013): Dominant roles of riverine discharge and sediment grain size. Geomorphology, 292: 115-127.

Wu, X., Bi, N., Syvitski, J., Saito, Y., Xu, J., Nittrouer, J.A., Bianchi, T.S., Yang, Z., Wang, H., 2020. Can reservoir regulation along the Yellow River be a sustainable way to save a sinking delta?. Earth's Future, 8(11): e2020EF001587.

Xia, J, Wu, B, Wang, G., Wang, Y., 2010. Estimation of bankfull discharge in the Lower

Yellow River using different approaches. Geomorphology, 117: 66-77.

Xie, C., Cui, B., Xie, T., Yu, S., Liu, Z., Chen, C., Ning, Z., Wang, Q., Zou, Y., Shao, X., 2020. Hydrological connectivity dynamics of tidal flat systems impacted by severe reclamation in the Yellow River Delta. Science of the Total Environment, 739:139860.

Yang, S.L., Milliman, J.D., Li, P., Xu, K., 2011. 50,000 dams later: Erosion of the Yangtze River and its delta. Global and Planetary Change, 75(1-2): 14-20.

Yang, Z., Ji, Y., Bi, N., Lei, K., Wang, H., 2011. Sediment transport off the Huanghe (Yellow River) delta and the adjacent Bohai Sea in winter and seasonal comparison. Estuarine, Coastal and Shelf Science, 93: 173-181.

Yu, Y., Wang, H., Shi, X., Ran, X., Cui, T., Qiao, S., Liu, Y., 2013. New discharge regime of the Huanghe (Yellow River): Causes and implications. Continental Shelf Research, 69: 62-72.

Yu, X., Ji, Z., Wang, K., Dou, S., Wang, W., Chen, S., 2020. Morphological changes of the Yellow River Estuary and key technology for its course stabilization. Yellow River, 42(9):66-71.

Zhang, S., Xia, J., Wan, Z., Li, J., 2019. Variations in planform and cross-sectional geometries of Qingshuigou channel in Yellow River estuary (1976-2016). Journal of Hydroelectric Engineering, 38(1): 65-76. (In Chinese)

Zheng, S., Han, S., Tan, G., Xia, J., Wu, B., Wang, K., Edmonds, D., 2018. Morphological adjustment of the Qingshuigou channel on the Yellow River Delta and factors controlling its avulsion. Catena, 166: 44-55.

Zhou, L., Liu, J, Saito, Y., Diao, S., Gao, M., Qiu, J., Xu, C., He, L., Ye, S., 2020. Sediment budget of the Yellow River delta during 1959-2012, estimated from morphological changes and accumulation rates. Marine Geology, 430:106363.

Zhou, Y.Y., Huang, H.Q., Nanson, G.C., Huang, C., Liu, G.H., 2015. Progradation of the Yellow (Huanghe) River Delta in response to the implementation of a basin-scale water regulation program. Geomorphology, 243: 65-74.